CPC(HEP & NP), 2010, **34**(2): 157–164 Chinese Physics C Vol. 34, No. 2, Feb., 2010

$\mathrm{B} \to \mathrm{K}_0^*(1430)\eta^{(\prime)}$ decays in the pQCD approach*

LIU Xin(刘新)[1;1)] ZHANG Zhi-Qing(张志清)[1,2] XIAO Zhen-Jun(肖振军)[1;2)]

[1] Department of Physics and Institute of Theoretical Physics, Nanjing Normal University, Nanjing 210097, China
[2] Department of Mathematics and Physics, Henan University of Technology, Zhengzhou 450052, China

Abstract Based on the assumption of two-quark structure of the scalar meson $\mathrm{K}_0^*(1430)$, we calculate the CP-averaged branching ratios for $\mathrm{B} \to \mathrm{K}_0^*(1430)\eta^{(\prime)}$ decays in the framework of the perturbative QCD (pQCD) approach here. We perform the evaluations in two scenarios for the scalar meson spectrum. We find that: (a) the pQCD predictions for $Br(\mathrm{B} \to \mathrm{K}_0^*(1430)\eta^{(\prime)})$ which are about 10^{-5}–10^{-6}, basically agree with the data within large theoretical uncertainty; (b) the agreement between the pQCD predictions and the data in Scenario I is better than that in Scenario II, which can be tested by the forthcoming LHC experiments; (c) the annihilation contributions play an important role for these considered decays.

Key words B meson, perturbative QCD approach, scalar meson, branching ratio

PACS 13.25.Hw, 12.38.Bx, 14.40.Nd

1 Introduction

Very recently, the branching ratios of $\mathrm{B} \to \mathrm{K}_0^*(1430)\eta$ decays have been measured by BaBar collaboration [1] with good precision:

$$\begin{aligned} Br(\mathrm{B}^+ \to \mathrm{K}_0^{*+}(1430)\eta) &= 18.2 \pm 2.6 \pm 2.6 \times 10^{-6}, \\ Br(\mathrm{B}^0 \to \mathrm{K}_0^{*0}(1430)\eta) &= 11.0 \pm 1.6 \pm 1.5 \times 10^{-6}. \end{aligned} \quad (1)$$

It is well-known that the underlying structure of scalar mesons is not well established theoretically (for a review, see e.g. Refs. [2–4]). Presently, motivated by the large number of B production and decay events expected at the forthcoming LHC experiments, the scalar meson spectrum is becoming one of the interesting topics for both experimental and theoretical studies. It is hoped that through the study of $\mathrm{B} \to \mathrm{SP}$ (S and P are scalar and pseudoscalar mesons) decays, old puzzles related to the internal structure and related parameters, e.g., the masses and widths, of light scalar mesons can receive new understanding. On one hand, $\mathrm{B} \to \mathrm{SP}$ is another window to study their properties [5, 6]; on the other hand, CP asymmetries of these decays provide another way to measure the CKM angles β and maybe α [7]. Additionally, $\mathrm{B} \to \mathrm{SP}$ decays have to be taken into account in order to analyze the $\mathrm{B} \to 3\mathrm{P}$ decays in the different channels [8] and perhaps these decays can be used to study new physics (NP) effects [9].

At present, some $\mathrm{B} \to \mathrm{SP}, \mathrm{SV}$ decays [6, 10, 11] have been studied, for example, by employing the QCD factorization (QCDF) approach [12] or the perturbative QCD (pQCD) approach [13–15]. In this paper, based on the assumption of two-quark structure of scalar K_0^* meson (For the sake of simplicity, we will use K_0^* to denote $\mathrm{K}_0^*(1430)$ in the following section), we will calculate the branching ratios for the four $\mathrm{B} \to \mathrm{K}_0^{*+}\eta, \mathrm{K}_0^{*+}\eta', \mathrm{K}_0^{*0}\eta$ and $\mathrm{K}_0^{*0}\eta'$ decays by employing the pQCD factorization approach.

This paper is organized as follows. In Sec. 2, we calculate analytically the related Feynman diagrams and present the various decay amplitudes for the studied decay modes. In Sec. 3, we show the numerical results for the branching ratios of $\mathrm{B} \to \mathrm{K}_0^*\eta^{(\prime)}$ decays. A short summary and some phenomenological discussions are also included in this section.

2 Perturbative calculations

Since the b quark is rather heavy we consider the B meson at rest for simplicity. It is convenient to use light-cone coordinate $(p^+, p^-, \boldsymbol{p}_\mathrm{T})$ to describe the me-

Received 14 April 2009
* Supported by National Natural Science Foundation of China (10575052, 10605012, 10735080)
1) E-mail: js.xin.liu@gmail.com
2) E-mail: xiaozhenjun@njnu.edu.cn

son's momenta. Using the light-cone coordinates the B meson and the two final state meson momenta can be written as

$$\begin{aligned} P_1 &= \frac{M_{\rm B}}{\sqrt{2}}(1,1,\mathbf{0}_{\rm T}),\\ P_2 &= \frac{M_{\rm B}}{\sqrt{2}}(1,0,\mathbf{0}_{\rm T}),\\ P_3 &= \frac{M_{\rm B}}{\sqrt{2}}(0,1,\mathbf{0}_{\rm T}), \end{aligned} \tag{2}$$

respectively, here the light meson masses have been neglected. Putting the light (anti-) quark momenta in B, η and $\rm K_0^*$ mesons as k_1, k_2, and k_3, respectively, we can choose

$$\begin{aligned} k_1 &= (x_1P_1^+,0,\boldsymbol{k}_{1\rm T}),\\ k_2 &= (x_2P_2^+,0,\boldsymbol{k}_{2\rm T}),\\ k_3 &= (0,x_3P_3^-,\boldsymbol{k}_{3\rm T}). \end{aligned} \tag{3}$$

Then, after the integration over k_1^-, k_2^-, and k_3^+, the decay amplitude for $\rm B^+\to K_0^{*+}\eta$ decay, for example, can be conceptually written as

$$\begin{aligned} \mathcal{A}(\mathrm{B}^+\to \mathrm{K}_0^{*+}\eta) \sim \int & \mathrm{d}x_1\mathrm{d}x_2\mathrm{d}x_3 b_1\mathrm{d}b_1 b_2\mathrm{d}b_2 b_3\mathrm{d}b_3\cdot \\ & \mathrm{Tr}\Big[C(t)\Phi_{\rm B}(x_1,b_1)\Phi_{\eta}(x_2,b_2)\times \\ & \Phi_{\mathrm{K}_0^*}(x_3,b_3)H(x_i,b_i,t)S_{\rm t}(x_i)\,\mathrm{e}^{-S(t)}\Big], \end{aligned} \tag{4}$$

where k_i are the momenta of light quarks included in each meson, the term Tr denotes the trace over Dirac and color indices, $C(t)$ is the Wilson coefficient evaluated at scale t, the hard kernel $H(k_1,k_2,k_3,t)$ is the hard part and can be calculated perturbatively, the function $\Phi_{\rm M}$ is the wave function, the function $S_{\rm t}(x_i)$ describes the threshold resummation [16] which smears the end-point singularities on x_i, and the last term, $\mathrm{e}^{-S(t)}$, is the Sudakov form factor which suppresses the soft dynamics effectively.

For the two-body charmless B meson decays, the related weak effective Hamiltonian $\mathcal{H}_{\rm eff}$ can be written as [17]

$$\begin{aligned} \mathcal{H}_{\rm eff} &= \frac{G_{\rm F}}{\sqrt{2}}\Bigg[V_{\rm ub}^*V_{\rm us}\left(C_1(\mu)O_1^u(\mu)+C_2(\mu)O_2^u(\mu)\right)- \\ & V_{\rm tb}^*V_{\rm ts}\sum_{i=3}^{10}C_i(\mu)\,O_i(\mu)\Bigg], \end{aligned} \tag{5}$$

where $C_i(\mu)$ are the Wilson coefficients at the renormalization scale μ and O_i are the four-fermion operators for the case of $\rm \bar{b}\to\bar{s}$ transition [17]. For the Wilson coefficients $C_i(\mu)$ $(i=1,\ldots,10)$, we will use the leading order (LO) expressions, although the next-to-leading order (NLO) results already exist in the literature [17]. This is the consistent way to cancel the explicit μ dependence in the theoretical formulae. For the renormalization group evolution of the Wilson coefficients from higher scale to lower scale, we use the formulae as given in Ref. [18] directly.

In the two-quark picture, the decay constants $f_{\rm K_0^*}$ and $\bar{f}_{\rm K_0^*}$ for a scalar meson $\rm K_0^*$ are defined by:

$$\langle K_0^*(p)|\bar{q}_2\gamma_\mu q_1|0\rangle = f_{\rm K_0^*}p_\mu,\ \ \langle K_0^*(p)|\bar{q}_2q_1|0\rangle = m_{\rm K_0^*}\bar{f}_{\rm K_0^*}, \tag{6}$$

where $m_{\rm K_0^*}(p)$ is the mass (momentum) of the scalar meson, and

$$f_{\rm K_0^*} = -0.025\pm0.002\ \mathrm{GeV},\ \ \bar{f}_{\rm K_0^*} = -0.300\pm0.030\ \mathrm{GeV} \tag{7}$$

in Scenario I, and

$$f_{\rm K_0^*} = 0.037\pm0.004\ \mathrm{GeV},\ \ \bar{f}_{\rm K_0^*} = 0.445\pm0.050\ \mathrm{GeV}, \tag{8}$$

in Scenario II [6], respectively.

The light-cone wave function of the scalar meson $\rm K_0^*$ is defined as:

$$\begin{aligned} \Phi_{\mathrm{K}_0^*,\alpha\beta} &= \frac{\mathrm{i}}{\sqrt{2N_{\rm C}}}\Big\{ \not{p}\phi_{\rm K_0^*}(x)+m_{\rm K_0^*}\phi^{\rm S}_{\rm K_0^*}(x)+ \\ & m_{\rm K_0^*}(\not{v}\,\not{n}-1)\phi^{\rm T}_{\rm K_0^*}(x)\Big\}_{\alpha\beta}, \end{aligned} \tag{9}$$

where $v=(0,1,\mathbf{0}_{\rm T})$ and $n=(1,0,\mathbf{0}_{\rm T})$ are the dimensionless light-like unit vectors.

The twist-2 light-cone distribution amplitude $\phi_{\rm K_0^*}(x,\mu)$ can be expanded as the Gegenbauer polynomials:

$$\begin{aligned} \phi_{\rm K_0^*}(x,\mu) &= \frac{3}{\sqrt{2N_{\rm c}}}x(1-x)\Big\{f_{\rm K_0^*}(\mu)+ \\ & \bar{f}_{\rm K_0^*}(\mu)\sum_{m=1}^{\infty}B_m(\mu)C_m^{3/2}(2x-1)\Big\}, \end{aligned} \tag{10}$$

where the values for Gegenbauer moments are taken at scale μ = 1 GeV [6]: $B_1=0.58\pm0.07$, $B_3=-1.20\pm0.08$ (Scenario I) and $B_1=-0.57\pm0.13$, $B_3=-0.42\pm0.22$ (Scenario II).

As for the twist-3 distribution amplitudes $\phi^{\rm S}_{\rm K_0^*}$ and $\phi^{\rm T}_{\rm K_0^*}$, we adopt the asymptotic form:

$$\phi^{\rm S}_{\rm K_0^*} = \frac{1}{2\sqrt{2N_{\rm c}}}\bar{f}_{\rm K_0^*},\quad \phi^{\rm T}_{\rm K_0^*} = \frac{1}{2\sqrt{2N_{\rm c}}}\bar{f}_{\rm K_0^*}(1-2x). \tag{11}$$

The B meson is treated as a heavy-light system. We here use the same B meson wave function as in Refs. [19, 20]. For the η-η′ system, we use the quark-flavor basis with $\eta_{\rm q}=(\rm u\bar{u}+d\bar{d})/\sqrt{2}$ and $\eta_{\rm s}=\rm s\bar{s}$, employ the same wave function, the identical distribution amplitudes $\phi^{\rm A,P,T}_{\eta_{\rm q,s}}$, and use the same values for other relevant input parameters, such as $f_{\rm q}=(1.07\pm0.02)f_\pi$, $f_{\rm s}=(1.34\pm0.06)f_\pi$, $\phi=39.3^\circ\pm1.0^\circ$, etc., as given in Ref. [21]. From those currently known studies [19, 20, 22] we believe that there is no large room left for the contribution due to the gluonic component of $\eta^{(\prime)}$, and therefore neglect the possible gluonic component in both η and η' meson.

We firstly take $\mathrm{B}^+\to\mathrm{K}_0^{*+}\eta$ decay mode as an example, and then extend our study to $\mathrm{B}^+\to\mathrm{K}_0^{*+}\eta'$ and $\mathrm{B}^0\to\mathrm{K}_0^{*0}\eta^{(\prime)}$ decays. Similar to the leading order $\mathrm{B}\to\mathrm{K}\eta^{(\prime)}$ decays in Ref. [23], there are 8 types of diagrams contributing to the $\mathrm{B}^+\to\mathrm{K}_0^{*+}\eta$ decays, as illustrated in Fig. 1. We first calculate the usual factorizable diagrams (a) and (b). Operators $O_{1-4,9,10}$ are $(V-A)(V-A)$ currents, the sum of their amplitudes is given as

$$F_{\mathrm{eK}_0^*} = 8\pi C_{\mathrm{F}} m_{\mathrm{B}}^2 \int_0^1 \mathrm{d}x_1\mathrm{d}x_3 \int_0^\infty b_1\mathrm{d}b_1 b_3\mathrm{d}b_3\, \phi_{\mathrm{B}}(x_1,b_1)\times \Big\{h_{\mathrm{e}}(x_1,x_3,b_1,b_3)\, E_{\mathrm{e}}(t_{\mathrm{a}})[(1+x_3)\phi_{\mathrm{K}_0^*}(x_3)+ r_{\mathrm{S}}(1-2x_3)(\phi^{\mathrm{S}}_{\mathrm{K}_0^*}(x_3)+\phi^{\mathrm{T}}_{\mathrm{K}_0^*}(x_3))]+ 2r_{\mathrm{S}}\phi^{\mathrm{S}}_{\mathrm{K}_0^*}(x_3)\, h_{\mathrm{e}}(x_3,x_1,b_3,b_1)\, E_{\mathrm{e}}(t_{\mathrm{b}})\Big\}, \tag{12}$$

where $r_{\mathrm{S}}=m_{\mathrm{K}_0^*}/m_{\mathrm{B}}$; $C_{\mathrm{F}}=4/3$ is a color factor.

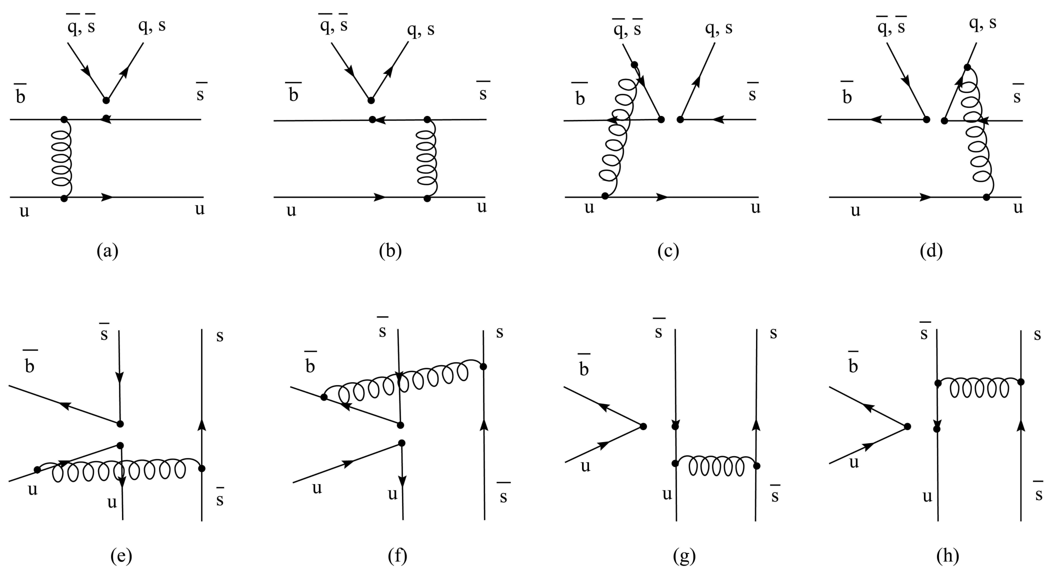

Fig. 1. Typical Feynman diagrams contributing to the $\mathrm{B}^+\to\mathrm{K}_0^{*+}\eta$ decays, where diagrams (a) and (b) contribute to the $\mathrm{B}\to\mathrm{K}_0^*$ form factor $\mathrm{F}_{0,1}^{\mathrm{B}\to\mathrm{K}_0^*}$.

The contributions from the operators $O_{5,6,7,8}$ can be written as

$$F^{\mathrm{P1}}_{\mathrm{eK}_0^*} = -F_{\mathrm{eK}_0^*}\,. \tag{13}$$

$$F^{\mathrm{P2}}_{\mathrm{eK}_0^*} = 16\pi C_{\mathrm{F}} m_{\mathrm{B}}^2 r_\eta \int_0^1 \mathrm{d}x_1\mathrm{d}x_3 \int_0^\infty b_1\mathrm{d}b_1 b_3\mathrm{d}b_3\, \phi_{\mathrm{B}}(x_1,b_1)\times \left\{ \left[\phi_{\mathrm{K}_0^*}(x_3)+r_{\mathrm{S}}[(2+x_3)\phi^{\mathrm{S}}_{\mathrm{K}_0^*}(x_3)-x_3\phi^{\mathrm{T}}_{\mathrm{K}_0^*}(x_3)]\right]\times h_{\mathrm{e}}(x_1,x_3,b_1,b_3)\, E_{\mathrm{e}}(t_{\mathrm{a}})+ 2r_{\mathrm{S}}\phi^{\mathrm{S}}_{\mathrm{K}_0^*}(x_3)\, h_{\mathrm{e}}(x_3,x_1,b_3,b_1)\, E_{\mathrm{e}}(t_{\mathrm{b}})\right\}, \tag{14}$$

where $r_\eta = m_0^{\eta_q}/m_{\mathrm{B}}$ and/or $r_\eta = m_0^{\eta_s}/m_{\mathrm{B}}$.

For the hard spectator diagrams 1(c) and 1(d), the corresponding decay amplitudes can be written as

$$M_{\mathrm{eK}_0^*} = \frac{32}{\sqrt{6}}\pi C_{\mathrm{F}} m_{\mathrm{B}}^2 \int_0^1 \mathrm{d}x_1\mathrm{d}x_2\,\mathrm{d}x_3\,\times \int_0^\infty b_1\mathrm{d}b_1 b_2\mathrm{d}b_2\, \phi_{\mathrm{B}}(x_1,b_1)\phi^{\mathrm{A}}_\eta(x_2)\times \left\{ \left[(1-x_2)\phi_{\mathrm{K}_0^*}(x_3)-r_{\mathrm{S}}x_3(\phi^{\mathrm{S}}_{\mathrm{K}_0^*}(x_3)-\phi^{\mathrm{T}}_{\mathrm{K}_0^*}(x_3))\right]\times E_{\mathrm{ne}}(t_{\mathrm{c}})h^{\mathrm{c}}_{\mathrm{ne}}(x_1,x_2,x_3,b_1,b_2)-h^{\mathrm{d}}_{\mathrm{ne}}(x_1,x_2,x_3,b_1,b_2)\times \left[(x_2+x_3)\phi_{\mathrm{K}_0^*}(x_3)-r_{\mathrm{S}}x_3(\phi^{\mathrm{S}}_{\mathrm{K}_0^*}(x_3)+ \phi^{\mathrm{T}}_{\mathrm{K}_0^*}(x_3))\right]E_{\mathrm{ne}}(t_{\mathrm{d}})\right\}, \tag{15}$$

$$
\begin{aligned}
M_{\mathrm{eK}_0^*}^{\mathrm{P1}} = & -\frac{32}{\sqrt{6}}\pi C_{\mathrm{F}} m_{\mathrm{B}}^2 \int_0^1 \mathrm{d}x_1 \mathrm{d}x_2\, \mathrm{d}x_3 \int_0^\infty b_1 \mathrm{d}b_1 b_2 \mathrm{d}b_2\, \phi_{\mathrm{B}}(x_1,b_1) r_\eta \Big\{ \Big[(1-x_2)\phi_{\mathrm{K}_0^*}(x_3)\times \\
& (\phi_\eta^{\mathrm{P}}(x_2)+\phi_\eta^{\mathrm{T}}(x_2)) - r_{\mathrm{S}} \Big(\phi_\eta^{\mathrm{P}}(x_2)[(1-x_2+x_3)\phi_{\mathrm{K}_0^*}^{\mathrm{S}}(x_3)-(1-x_2-x_3)\phi_{\mathrm{K}_0^*}^{\mathrm{T}}(x_3)] + \\
& \phi_\eta^{\mathrm{T}}(x_2)[(1-x_2-x_3)\phi_{\mathrm{K}_0^*}^{\mathrm{S}}(x_3)-(1-x_2+x_3)\phi_{\mathrm{K}_0^*}^{\mathrm{T}}] \Big) \Big] h_{\mathrm{ne}}^{\mathrm{c}}(x_1,x_2,x_3,b_1,b_2) E_{\mathrm{ne}}(t_{\mathrm{c}}) - \\
& \Big[x_2(\phi_\eta^{\mathrm{P}}(x_2)-\phi_\eta^{\mathrm{T}}(x_2))\phi_{\mathrm{K}_0^*}(x_3) + r_{\mathrm{S}}(x_2(\phi_\eta^{\mathrm{P}}(x_2)-\phi_\eta^{\mathrm{T}}(x_2))(\phi_{\mathrm{K}_0^*}^{\mathrm{S}}(x_3)-\phi_{\mathrm{K}_0^*}^{\mathrm{T}}(x_3)) + \\
& x_3(\phi_\eta^{\mathrm{P}}(x_2)+\phi_\eta^{\mathrm{T}}(x_2))(\phi_{\mathrm{K}_0^*}^{\mathrm{S}}(x_3)+\phi_{\mathrm{K}_0^*}^{\mathrm{T}}(x_3))) \Big] E_{\mathrm{ne}}(t_{\mathrm{d}}) h_{\mathrm{ne}}^{\mathrm{d}}(x_1,x_2,x_3,b_1,b_2) \Big\}, \qquad (16)
\end{aligned}
$$

$$
\begin{aligned}
M_{\mathrm{eK}_0^*}^{\mathrm{P2}} = & -\frac{32}{\sqrt{6}}\pi C_{\mathrm{F}} m_{\mathrm{B}}^2 \int_0^1 \mathrm{d}x_1 \mathrm{d}x_2\, \mathrm{d}x_3 \int_0^\infty b_1 \mathrm{d}b_1 b_2 \mathrm{d}b_2\, \phi_{\mathrm{B}}(x_1,b_1) \phi_\eta^{\mathrm{A}}(x_2) \Big\{ E_{\mathrm{ne}}(t_{\mathrm{c}})\times \\
& \Big[(1-x_2+x_3)\phi_{\mathrm{K}_0^*}(x_3) - r_{\mathrm{S}} x_3(\phi_{\mathrm{K}_0^*}^{\mathrm{S}}(x_3)+\phi_{\mathrm{K}_0^*}^{\mathrm{T}}(x_3)) \Big] h_{\mathrm{ne}}^{\mathrm{c}}(x_1,x_2,x_3,b_1,b_2) - \\
& \Big[x_2\phi_{\mathrm{K}_0^*}(x_3) - r_{\mathrm{S}} x_3(\phi_{\mathrm{K}_0^*}^{\mathrm{S}}(x_3)-\phi_{\mathrm{K}_0^*}^{\mathrm{T}}(x_3)) \Big] E_{\mathrm{ne}}(t_{\mathrm{d}}) h_{\mathrm{ne}}^{\mathrm{d}}(x_1,x_2,x_3,b_1,b_2) \Big\}. \qquad (17)
\end{aligned}
$$

For the non-factorizable annihilation diagrams 1(e) and 1(f), we find

$$
\begin{aligned}
M_{\mathrm{aK}_0^*} = & \frac{32}{\sqrt{6}}\pi C_{\mathrm{F}} m_{\mathrm{B}}^2 \int_0^1 \mathrm{d}x_1 \mathrm{d}x_2\, \mathrm{d}x_3 \int_0^\infty b_1 \mathrm{d}b_1 b_2 \mathrm{d}b_2\, \phi_{\mathrm{B}}(x_1,b_1) \Big\{ \Big[(1-x_3)\phi_\eta^{\mathrm{A}}(x_2)\phi_{\mathrm{K}_0^*}(x_3) - \\
& r_\eta r_{\mathrm{S}} \Big(\phi_\eta^{\mathrm{P}}(x_2) \Big[(1+x_2-x_3)\phi_{\mathrm{K}_0^*}^{\mathrm{S}}(x_3)-(1-x_2-x_3)\phi_{\mathrm{K}_0^*}^{\mathrm{T}}(x_3) \Big] + \phi_\eta^{\mathrm{T}}(x_2)\times \\
& \Big[(1-x_2-x_3)\phi_{\mathrm{K}_0^*}^{\mathrm{S}}(x_3)-(1+x_2-x_3)\phi_{\mathrm{K}_0^*}^{\mathrm{T}}(x_3) \Big] \Big) \Big] E_{\mathrm{na}}(t_{\mathrm{e}}) h_{\mathrm{na}}^{\mathrm{e}}(x_1,x_2,x_3,b_1,b_2) - \\
& \Big[x_2\phi_\eta^{\mathrm{A}}(x_2)\phi_{\mathrm{K}_0^*}(x_3) - r_\eta r_{\mathrm{S}} \Big(\phi_\eta^{\mathrm{P}}(x_2)[(3+x_2-x_3)\phi_{\mathrm{K}_0^*}^{\mathrm{S}}(x_3)+(1-x_2-x_3)\times \\
& \phi_{\mathrm{K}_0^*}^{\mathrm{T}}(x_3)] + \phi_\eta^{\mathrm{T}}(x_2)[(-1+x_2+x_3)\phi_{\mathrm{K}_0^*}^{\mathrm{S}}(x_3)+(1-x_2+x_3)\phi_{\mathrm{K}_0^*}^{\mathrm{T}}(x_3)] \Big) \Big] \times \\
& E_{\mathrm{na}}(t_{\mathrm{f}}) h_{\mathrm{na}}^{\mathrm{f}}(x_1,x_2,x_3,b_1,b_2) \Big\}, \qquad (18)
\end{aligned}
$$

$$
\begin{aligned}
M_{\mathrm{aK}_0^*}^{\mathrm{P1}} = & -\frac{32}{\sqrt{6}}\pi C_{\mathrm{F}} m_{\mathrm{B}}^2 \int_0^1 \mathrm{d}x_1 \mathrm{d}x_2\, \mathrm{d}x_3 \int_0^\infty b_1 \mathrm{d}b_1 b_2 \mathrm{d}b_2\, \phi_{\mathrm{B}}(x_1,b_1) \Big\{ \Big[r_\eta x_2 \phi_{\mathrm{K}_0^*}(x_3)(\phi_\eta^{\mathrm{P}}(x_2)+ \\
& \phi_\eta^{\mathrm{T}}(x_2)) + r_{\mathrm{S}}(1-x_3)\phi_\eta^{\mathrm{A}}(x_2)(\phi_{\mathrm{K}_0^*}^{\mathrm{S}}(x_3)-\phi_{\mathrm{K}_0^*}^{\mathrm{T}}(x_3)) \Big] E_{\mathrm{na}}(t_{\mathrm{e}}) h_{\mathrm{na}}^{\mathrm{e}}(x_1,x_2,x_3,b_1,b_2) + \\
& \Big[r_\eta(2-x_2)(\phi_\eta^{\mathrm{P}}(x_2)+\phi_\eta^{\mathrm{T}}(x_2))\phi_{\mathrm{K}_0^*}(x_3) + r_{\mathrm{S}}(1+x_3)(\phi_{\mathrm{K}_0^*}^{\mathrm{S}}(x_3)-\phi_{\mathrm{K}_0^*}^{\mathrm{T}}(x_3))\times \\
& \phi_\eta^{\mathrm{A}}(x_2) \Big] E_{\mathrm{na}}(t_{\mathrm{f}}) h_{\mathrm{na}}^{\mathrm{f}}(x_1,x_2,x_3,b_1,b_2) \Big\}, \qquad (19)
\end{aligned}
$$

For the factorizable annihilation diagrams 1(g) and 1(h), we have

$$
\begin{aligned}
F_{\mathrm{aK}_0^*} = & 8 f_{\mathrm{B}} \pi C_{\mathrm{F}} m_{\mathrm{B}}^2 \int_0^1 \mathrm{d}x_2 \mathrm{d}x_3 \int_0^\infty b_2 \mathrm{d}b_2 b_3 \mathrm{d}b_3 \Big\{ \Big[x_2\phi_\eta^{\mathrm{A}}(x_2)\phi_{\mathrm{K}_0^*}(x_3) - 2 r_\eta r_{\mathrm{S}} \times \\
& \big((x_2+1)\phi_\eta^{\mathrm{P}}(x_2) + (x_2-1)\phi_\eta^{\mathrm{T}}(x_2) \big) \phi_{\mathrm{K}_0^*}^{\mathrm{S}}(x_3) \Big] h_{\mathrm{a}}(x_2,1-x_3,b_2,b_3)\times \\
& E_{\mathrm{a}}(t_{\mathrm{g}}) + \Big[(x_3-1)\phi_\eta^{\mathrm{A}}(x_2)\phi_{\mathrm{K}_0^*}(x_3) - 2 r_\eta r_{\mathrm{S}} \phi_\eta^{\mathrm{P}}(x_2) \Big((x_3-2)\phi_{\mathrm{K}_0^*}^{\mathrm{S}}(x_3) - \\
& x_3\phi_{\mathrm{K}_0^*}^{\mathrm{T}}(x_3) \Big) \Big] E_{\mathrm{a}}(t_{\mathrm{h}}) h_{\mathrm{a}}(1-x_3,x_2,b_3,b_2) \Big\}, \qquad (20)
\end{aligned}
$$

$$F^{\mathrm{P2}}_{\mathrm{aK}_0^*} = 16 f_{\mathrm{B}}\pi C_{\mathrm{F}} m_{\mathrm{B}}^2 \int_0^1 \mathrm{d}x_2\mathrm{d}x_3 \int_0^\infty b_2\mathrm{d}b_2 b_3\mathrm{d}b_3 \Big\{\Big[2r_{\mathrm{S}}\phi_\eta^{\mathrm{A}}(x_2)\phi^{\mathrm{S}}_{\mathrm{K}_0^*}(x_3) - r_\eta x_2(\phi_\eta^{\mathrm{P}}(x_2)-\phi_\eta^{\mathrm{T}}(x_2))\phi_{\mathrm{K}_0^*}(x_3)\Big] h_{\mathrm{a}}(x_2,1-x_3,b_2,b_3)E_{\mathrm{a}}(t_{\mathrm{g}}) + \Big[r_{\mathrm{S}}(1-x_3)\phi_\eta^{\mathrm{A}}(x_2)(\phi^{\mathrm{S}}_{\mathrm{K}_0^*}(x_3)+\phi^{\mathrm{T}}_{\mathrm{K}_0^*}(x_3)) - 2r_\eta\phi_\eta^{\mathrm{P}}(x_2)\phi_{\mathrm{K}_0^*}(x_3)\Big] \times E_{\mathrm{a}}(t_{\mathrm{h}})h_{\mathrm{a}}(1-x_3,x_2,b_3,b_2)\Big\}. \quad (21)$$

For the $\mathrm{B}^+\to\mathrm{K}_0^{*+}\eta$ decay, besides the Feynman diagrams as shown in Fig. 1 where the upper emitted meson is the η, the Feynman diagrams obtained by exchanging the position of K_0^{*+} and η also contribute to this decay mode. The decays amplitudes for the first four new diagrams can be obtained by the replacements

$$\phi_{\mathrm{K}_0^*}\longleftrightarrow\phi_\eta^{\mathrm{A}},\quad \phi^{\mathrm{S}}_{\mathrm{K}_0^*}\longleftrightarrow\phi_\eta^{\mathrm{P}},\quad \phi^{\mathrm{T}}_{\mathrm{K}_0^*}\longleftrightarrow\phi_\eta^{\mathrm{T}},\quad r_{\mathrm{S}}\longleftrightarrow r_\eta. \quad (22)$$

For the last four annihilation diagrams, the decay amplitudes can be written as,

$$M_{\mathrm{a}\eta} = \frac{32}{\sqrt{6}}\pi C_{\mathrm{F}} m_{\mathrm{B}}^2 \int_0^1 \mathrm{d}x_1\mathrm{d}x_2\,\mathrm{d}x_3 \int_0^\infty b_1\mathrm{d}b_1 b_2\mathrm{d}b_2\,\phi_{\mathrm{B}}(x_1,b_1)\Big\{\Big[(1-x_3)\phi_{\mathrm{K}_0^*}(x_2)\phi_\eta^{\mathrm{A}}(x_3) + r_\eta r_{\mathrm{S}}\Big(\phi^{\mathrm{S}}_{\mathrm{K}_0^*}(x_2)[(1+x_2-x_3)\phi_\eta^{\mathrm{P}}(x_3)-(1-x_2-x_3)\phi_\eta^{\mathrm{T}}(x_3)] + \phi^{\mathrm{T}}_{\mathrm{K}_0^*}(x_2)[\phi_\eta^{\mathrm{P}}(x_3)\times(1-x_2-x_3)-(1+x_2-x_3)\phi_\eta^{\mathrm{T}}(x_3)]\Big)\Big] h^{\mathrm{e}}_{\mathrm{na}}(x_1,x_2,x_3,b_1,b_2)E_{\mathrm{na}}(t_{\mathrm{e}}) - E_{\mathrm{na}}(t_{\mathrm{f}})\times \Big[x_2\phi_{\mathrm{K}_0^*}(x_2)\phi_\eta^{\mathrm{A}}(x_3) + r_\eta r_{\mathrm{S}}\Big(\phi^{\mathrm{S}}_{\mathrm{K}_0^*}(x_2)[(3+x_2-x_3)\phi_\eta^{\mathrm{P}}(x_3)+(1-x_2-x_3)\phi_\eta^{\mathrm{T}}(x_3)] - \phi^{\mathrm{T}}_{\mathrm{K}_0^*}(x_2)[(1-x_2-x_3)\phi_\eta^{\mathrm{P}}(x_3)-(1-x_2+x_3)\phi_\eta^{\mathrm{T}}(x_3)]\Big)\Big] h^{\mathrm{f}}_{\mathrm{na}}(x_1,x_2,x_3,b_1,b_2)\Big\}, \quad (23)$$

$$M^{\mathrm{P1}}_{\mathrm{a}\eta} = \frac{32}{\sqrt{6}}\pi C_{\mathrm{F}} m_{\mathrm{B}}^2 \int_0^1 \mathrm{d}x_1\mathrm{d}x_2\,\mathrm{d}x_3 \int_0^\infty b_1\mathrm{d}b_1 b_2\mathrm{d}b_2\,\phi_{\mathrm{B}}(x_1,b_1)\Big\{\Big[r_{\mathrm{S}}x_2(\phi^{\mathrm{S}}_{\mathrm{K}_0^*}(x_2)+\phi^{\mathrm{T}}_{\mathrm{K}_0^*}(x_2))\times \phi_\eta^{\mathrm{A}}(x_3) - r_\eta(1-x_3)\phi_{\mathrm{K}_0^*}(x_2)(\phi_\eta^{\mathrm{P}}(x_3)-\phi_\eta^{\mathrm{T}}(x_3))\Big] E_{\mathrm{na}}(t_{\mathrm{e}})h^{\mathrm{e}}_{\mathrm{na}}(x_1,x_2,x_3,b_1,b_2) + \Big[r_{\mathrm{S}}(2-x_2)(\phi^{\mathrm{S}}_{\mathrm{K}_0^*}(x_2)+\phi^{\mathrm{T}}_{\mathrm{K}_0^*}(x_2))\phi_\eta^{\mathrm{A}}(x_3) - r_\eta(1+x_3)\phi_{\mathrm{K}_0^*}(x_2)(\phi_\eta^{\mathrm{P}}(x_3)-\phi_\eta^{\mathrm{T}}(x_3))\Big] \times E_{\mathrm{na}}(t_{\mathrm{f}})h^{\mathrm{f}}_{\mathrm{na}}(x_1,x_2,x_3,b_1,b_2)\Big\}, \quad (24)$$

$$F_{\mathrm{a}\eta} = 8 f_{\mathrm{B}}\pi C_{\mathrm{F}} m_{\mathrm{B}}^2 \int_0^1 \mathrm{d}x_2\mathrm{d}x_3 \int_0^\infty b_2\mathrm{d}b_2 b_3\mathrm{d}b_3 \Big\{\Big[x_2\phi_{\mathrm{K}_0^*}(x_2)\phi_\eta^{\mathrm{A}}(x_3) + 2r_\eta r_{\mathrm{S}}\times \Big((x_2+1)\phi^{\mathrm{S}}_{\mathrm{K}_0^*}(x_2)+(x_2-1)\phi^{\mathrm{T}}_{\mathrm{K}_0^*}(x_2)\Big)\phi_\eta^{\mathrm{P}}(x_3)\Big] E_{\mathrm{a}}(t_{\mathrm{g}})h_{\mathrm{a}}(x_2,1-x_3,b_2,b_3) - \Big[(1-x_3)\phi_{\mathrm{K}_0^*}(x_2)\phi_\eta^{\mathrm{A}}(x_3) + 2r_\eta r_{\mathrm{S}}\phi^{\mathrm{S}}_{\mathrm{K}_0^*}(x_2)\big((2-x_3)\phi_\eta^{\mathrm{P}}(x_3)+x_3\phi_\eta^{\mathrm{T}}(x_3)\big)\Big] \times E_{\mathrm{a}}(t_{\mathrm{h}})h_{\mathrm{a}}(1-x_3,x_2,b_3,b_2)\Big\}, \quad (25)$$

$$F^{\mathrm{P2}}_{\mathrm{a}\eta} = 16 f_{\mathrm{B}}\pi C_{\mathrm{F}} m_{\mathrm{B}}^2 \int_0^1 \mathrm{d}x_2\mathrm{d}x_3 \int_0^\infty b_2\mathrm{d}b_2 b_3\mathrm{d}b_3 \Big\{\Big[2r_\eta\phi_{\mathrm{K}_0^*}(x_2)\phi_\eta^{\mathrm{P}}(x_3) - r_{\mathrm{S}}x_2\phi_\eta^{\mathrm{A}}(x_3)\times (\phi^{\mathrm{S}}_{\mathrm{K}_0^*}(x_2)-\phi^{\mathrm{T}}_{\mathrm{K}_0^*}(x_2))\Big] h_{\mathrm{a}}(x_2,1-x_3,b_2,b_3)E_{\mathrm{a}}(t_{\mathrm{g}}) + h_{\mathrm{a}}(1-x_3,x_2,b_3,b_2)\times E_{\mathrm{a}}(t_{\mathrm{h}})\Big[2r_{\mathrm{S}}\phi^{\mathrm{S}}_{\mathrm{K}_0^*}(x_2)\phi_\eta^{\mathrm{A}}(x_3) + r_\eta(1-x_3)\phi_{\mathrm{K}_0^*}(x_2)(\phi_\eta^{\mathrm{P}}(x_3)+\phi_\eta^{\mathrm{T}}(x_3))\Big]\Big\}. \quad (26)$$

The explicit expressions of hard functions $E_{\mathrm{e,ne;na,a}}(t_i)$ and $h_{\mathrm{e,ne;na,a}}(x_i,b_j),\cdots$ can be found for example in Refs. [19, 20, 23].

Before writing the total amplitude of $B^+ \to K_0^{*+}\eta$ decay, we firstly define the combinations of Wilson coefficients as usual [24],

$$a_1 = C_2 + C_1/3, \quad a_2 = C_1 + C_2/3, \quad a_i = C_i + C_{i\pm 1}/3, \quad i = 3\text{–}10, \tag{27}$$

where the upper (lower) sign applies, when i is odd (even).

By combining the contributions from different diagrams, the total decay amplitudes for $B^+ \to K_0^{*+}\eta$, for example, can be written as

$$\begin{aligned}\mathcal{M}(K_0^{*+}\eta) = {}& \zeta_q F_{eK_0^*} f_q \left\{\lambda_u a_2 - \lambda_t\left[2(a_3-a_5) - \frac{1}{2}(a_7-a_9)\right]\right\} - \zeta_s f_s \lambda_t \left\{F_{eK_0^*} \times\right. \\ & \left[a_3+a_4-a_5+\frac{1}{2}(a_7-a_9-a_{10})\right] + F^{P2}_{eK_0^*}\left(a_6 - \frac{1}{2}a_8\right)\Big\} + \zeta_q\Big\{M_{eK_0^*} \times \\ & \left[\lambda_u C_2 - \lambda_t(2C_4 + \frac{1}{2}C_{10})\right] - M^{P2}_{eK_0^*}\lambda_t(2C_6+\frac{1}{2}C_8)\Big\} - \zeta_s\lambda_t\Big\{M_{eK_0^*}\times \\ & (C_3+C_4-\frac{1}{2}(C_9+C_{10})) + M^{P1}_{eK_0^*}(C_5-\frac{1}{2}C_7) + M^{P2}_{eK_0^*}(C_6-\frac{1}{2}C_8)\Big\} + \\ & \zeta_s\Big\{M_{aK_0^*}[\lambda_u C_1 - \lambda_t(C_3+C_9)] - M^{P1}_{aK_0^*}\lambda_t(C_5+C_7) - F^{P2}_{aK_0^*}\lambda_t(a_6 + \\ & a_8) + F_{aK_0^*}[\lambda_u a_1 - \lambda_t(a_4+a_{10})]\Big\} + \zeta_q\Big\{(f_{K_0^*}F_{e\eta_q} + F_{a\eta_q})[\lambda_u a_1 - \\ & \lambda_t(a_4+a_{10})] - (\bar{f}_{K_0^*}F^{P2}_{e\eta_q} + F^{P2}_{a\eta_q})\lambda_t(a_6+a_8) + (M_{e\eta_q}+M_{a\eta_q}) \times \\ & [\lambda_u C_1 - \lambda_t(C_3+C_9)] - (M^{P1}_{e\eta_q} + M^{P1}_{a\eta_q})\lambda_t(C_5+C_7)\Big\},\end{aligned} \tag{28}$$

where $\lambda_u = V_{ub}^* V_{us}$, $\lambda_t = V_{tb}^* V_{ts}$ and $\zeta_{q(s)} = \dfrac{\cos\phi}{\sqrt{2}}(-\sin\phi)$ for $\eta_q(\eta_s)$ with the flavor mixing angle $\phi = 39.3°$. For $B^0 \to K_0^{*0}\eta$ decay, we find the similar result.

For $B \to K_0^*\eta'$ channels, the total decay amplitudes can be easily obtained by replacing $\zeta_{q(s)}$ with $\zeta'_{q(s)} = \dfrac{\sin\phi}{\sqrt{2}}(\cos\phi)$ for $\eta'_q(\eta'_s)$ in Eq. (28).

3 Numerical results and discussions

In this section, we will calculate the CP-averaged branching ratios for those considered decay modes. The input parameters to be used are given in Appendix A. In numerical calculations, the central values of input parameters will be used implicitly unless otherwise stated.

Firstly, we find the pQCD predictions for the corresponding form factors at zero momentum transfer:

$$F_{0,1}^{B\to K_0^*}(q^2=0) = -0.44^{+0.06}_{-0.07}(\omega_b)^{+0.04}_{-0.04}(\bar{f}_{K_0^*})^{+0.02}_{-0.02}(B_{1,3}), \quad \text{(Scenario I)}$$

$$F_{0,1}^{B\to K_0^*}(q^2=0) = +0.76^{+0.12}_{-0.10}(\omega_b)^{+0.08}_{-0.08}(\bar{f}_{K_0^*})^{+0.07}_{-0.07}(B_{1,3}), \quad \text{(Scenario II)} \tag{29}$$

for $f_B = 0.19$ GeV, and $\omega_b = 0.40 \pm 0.04$ GeV. They agree well with those as given in Ref. [25].

Using the decay amplitudes obtained in last section, it is straightforward to calculate the branching ratios. The leading order pQCD predictions for the CP-averaged branching ratios in Scenario I are the following (in unit of 10^{-6})

$$Br(B^+ \to K_0^{*+}\eta) = 11.8^{+5.3+0.3+1.1+2.5}_{-3.5-0.4-1.2-2.3}(19.2), \tag{30}$$

$$Br(B^+ \to K_0^{*+}\eta') = 21.6^{+1.6+3.1+4.0+4.5}_{-0.5-2.8-3.6-4.1}(15.4), \tag{31}$$

$$Br(B^0 \to K_0^{*0}\eta) = 9.1^{+4.4+0.0+1.1+2.0}_{-2.8-0.1-1.1-1.8}(17.0), \tag{32}$$

$$Br(B^0 \to K_0^{*0}\eta') = 22.0^{+1.6+3.2+3.9+4.6}_{-0.5-3.6-3.0-4.2}(15.0), \tag{33}$$

and in Scenario II,

$$Br(B^+ \to K_0^{*+}\eta) = 33.8^{+13.5+1.1+7.7+8.2}_{-9.0-1.1-7.0-7.3}(38.8), \tag{34}$$

$$Br(B^+ \to K_0^{*+}\eta') = 77.5^{+15.8+6.2+21.0+18.0}_{-10.8-5.8-16.5-16.1}(49.6), \tag{35}$$

$$Br(B^0 \to K_0^{*0}\eta) = 28.4^{+11.6+1.4+6.4+6.9}_{-7.8-1.4-5.9-6.2}(34.2), \tag{36}$$

$$Br(B^0 \to K_0^{*0}\eta') = 74.2^{+15.0+6.4+20.5+17.2}_{-10.3-5.7-16.2-15.5}(48.2), \tag{37}$$

where the numbers in parentheses are the central values of branching ratios without the inclusion of annihilation diagrams. The first theoretical error is induced by the uncertainty of $\omega_b = 0.40 \pm 0.04$ GeV. The second uncertainty arises from the Gegenbauer moment $a_2^{\eta^{(\prime)}} = 0.115 \pm 0.115$. The last two errors are from the combinations of Gegenbauer coefficients B_1 and/or B_3 and decay constants $f_{K_0^*}$ and/or $\bar{f}_{K_0^*}$ of the scalar meson K_0^*, respectively.

Now some phenomenological discussions are in order:

(1) In the evaluations of $B \to K_0^*\eta^{(\prime)}$ modes, the updated parameters in the distribution amplitudes of $\eta^{(\prime)}$ mesons, for example, $a_2^{\eta^{(\prime)}} = 0.115 \pm 0.015$ and $a_4^{\eta^{(\prime)}} = -0.015$ were used.

(2) From the branching ratios for $B \to K_0^*\eta^{(\prime)}$ decays as shown in Eqs. (30–37), one can see that the results in Scenario II are nearly 3-4 times large as those in Scenario I for $B \to K_0^*\eta$ and $B \to K_0^*\eta'$ decays, respectively. This is because the decay constants in Scenario II are larger and sign-flipped, which results in the large branching ratios in Scenario II. The pQCD predictions in Scenario I are preferable by the existing data than in Scenario II.

(3) As shown in Eqs. (30–37), the annihilation diagrams play a more important role in contributing to the branching ratios in Scenario I than that in Scenario II for $B \to K_0^*\eta$, while the situation for $B \to K_0^*\eta'$ is quite the contrary. By neglecting the annihilation contributions, for example, the pQCD prediction for the central value of $Br(B^+ \to K_0^{*+}\eta)$ is from 11.8×10^{-6} to 19.2×10^{-6} in Scenario I while from 33.8×10^{-6} to 38.8×10^{-6} in Scenario II; the prediction for $Br(B^+ \to K_0^{*+}\eta')$ will change from 21.6×10^{-6} to 15.4×10^{-6} in Scenario I, the corresponding change, however, is from 77.5×10^{-6} to 49.6×10^{-6} in Scenario II.

(4) The long distance re-scattering effects may also affect the branching ratios of $B \to SP$. We here do not consider such effects since it is still very difficult to estimate them reliably now.

It is worth mentioning that the authors of Refs. [6, 10] have studied four $B \to K_0^*\pi$ decays by employing the QCDF and pQCD approach, respectively. They found that Scenario II is more preferable than Scenario I by comparing with the data. But the numerical results of branching ratios are very different in those two papers.

We also performed the calculations for the four $B \to K_0^*\pi$ decays in the pQCD approach, and confirmed that the large branching ratios could be obtained if the old Gegenbauer moments [26], i.e., $a_2^\pi = 0.44$ and $a_4^\pi = 0.25$, are used. By using the updated values of $a_2^\pi = 0.115 \pm 0.115$ and $a_4^\pi = -0.015$, we find that the corresponding pQCD predictions for the branching ratios of $B \to K_0^*\pi$ decays are decreased significantly by around 40% (see Table 1) in both scenarios.

Frankly speaking, the theoretical predictions for the branching ratios of all considered $B \to SP$ decays still have a very large parameter-dependence. we can not determine with enough confidence which scenario is the better one at present. Much more theoretical studies and larger data sample are required to understand the structure of scalar meson.

Table 1. The pQCD predictions for the branching ratios (in unit of 10^{-6}) for $B \to K_0^*\pi$ decays, obtained by using the new Gegenbauer moments in present work or the old ones in Ref. [10] respectively, where the various errors have been added in quadrature. By comparison, we also cite the measured values as given in Refs. [27, 28].

modes	Scenario I	Scenario II	Scenario I [10]	Scenario II [10]	data
$B^+ \to K_0^{*+}\pi^0$	$7.8^{+2.8}_{-2.3}$	$21.6^{+8.5}_{-6.6}$	$11.3^{+2.5}_{-2.2}$	$28.8^{+7.8}_{-7.3}$	–
$B^0 \to K_0^{*0}\pi^0$	$5.8^{+1.7}_{-1.5}$	$10.7^{+4.1}_{-3.2}$	$10.0^{+2.4}_{-2.2}$	$18.4^{+6.1}_{-5.1}$	$11.7^{+4.2}_{-3.8}$ [27]
$B^+ \to K_0^{*0}\pi^+$	$13.6^{+4.2}_{-3.6}$	$30.9^{+12.4}_{-9.2}$	$20.7^{+4.7}_{-4.3}$	$47.6^{+13.8}_{-11.9}$	47.0 ± 5.0 [28]
$B^0 \to K_0^{*+}\pi^-$	$13.2^{+4.0}_{-3.4}$	$31.6^{+12.4}_{-9.3}$	$20.0^{+4.6}_{-4.2}$	$43.0^{+12.8}_{-10.9}$	$50.0^{+8.0}_{-9.0}$ [28]

In short, we calculated the branching ratios for $B \to K_0^*\eta^{(\prime)}$ decays by using the pQCD factorization approach at leading order. We perform the evaluations in two scenarios for the scalar meson spectrum. Besides the usual factorizable diagrams, the non-factorizable and annihilation diagrams are also calculated analytically in the pQCD approach. we find that (a) the pQCD predictions for $Br(B \to K_0^*(1430)\eta^{(\prime)})$ which are about $10^{-5} - 10^{-6}$, basically agree with the data, but the theoretical error is still large; (b) the agreement between the pQCD predictions and the data in Scenario I is better than that in Scenario II, which can be tested by the forthcoming LHC experiments; (c) the annihilation contributions play an important role for these considered decays; (d) much more theoretical studies and larger data sample are needed to have a better understanding about the structure of scalar mesons.

X. Liu would like to thank Run-Hui Li for useful discussions.

Appendix A

Input parameters and wave functions

The masses, decay constants, QCD scales and B meson lifetime used in the calculations are

$$\Lambda^{(f=4)}_{\overline{\rm MS}} = 0.250 \text{ GeV}, \quad f_\pi = 0.130 \text{ GeV},$$

$$f_{\rm B} = 0.190 \text{ GeV}, \quad m_{{\rm K}_0^*} = 1.425 \text{ GeV},$$

$$m_0^{\eta_q} = 1.07 \text{ GeV}, \quad m_0^{\eta_s} = 1.92 \text{ GeV},$$

$$\tau_{\rm B^\pm} = 1.638\times 10^{-12} \text{ s}, \quad M_{\rm W} = 80.41 \text{ GeV},$$

$$M_{\rm B} = 5.28 \text{ GeV}, \quad \tau_{\rm B^0} = 1.53\times 10^{-12} \text{ s}.$$

For the CKM matrix elements, here we adopt the Wolfenstein parametrization for the CKM matrix, and take $\lambda = 0.2257$, $A = 0.814$, $\bar{\rho} = 0.135$ and $\bar{\eta} = 0.349$ [28].

References

1 Aubert B et al.(BABAR Collaboration). Phys. Rev. Lett., 2006, **97**: 201802
2 Spanier S, Tönqvist N A (Particle Data Group). Phys. Lett. B, 2008, **667**: 594–597; Amsler C et al. Phys. Lett. B, 2008, **667**: 1
3 Godfrey S, Napolitano J. Rev. Mod. Phys., 1999, **71**: 1411
4 Close F E, Tönqvist N A. J. Phys. G, 2002, **28**: R249
5 Delepine D, Lucio M J L, Ramirez C A. Eur. Phys. J. C, 2006, **45**: 693
6 CHENG H Y, CHUA C K, YANG K C. Phys. Rev. D, 2006, **73**: 014017
7 Sciolla G (BABAR collaboration). Nucl. Phys. Proc. Suppl., 2006, **156**: 16 ; Laplace S, Shelkov V. Eur. Phys. J. C, 2001, **22**: 431; Suzuki M. Phys. Rev. D, 2002, **65**: 097501; Dighe A S, Kim C S. Phys. Rev. D, 2000, **62**: 111302
8 El-Bennich B, Furman A, Kaminski R et al. Phys. Rev. D, 2006, **74**: 114009
9 Giri A K, Mawlong B, Mohanta R. Phys. Rev. D, 2006, **74**: 114001
10 SHEN Y L, WANG W, ZHU J, LÜ C D. Eur. Phys. J. C, 2007, **50**: 877
11 CHENG H Y, CHUA C K, YANG K C. Phys. Rev. D, 2008, **77**: 014034
12 Beneke M, Buchalla G, Neubert M, Sachrajda C T. Phys. Rev. Lett., 1999, **83**: 1914
13 CHANG C H V, LI H N. Phys. Rev. D, 1997, **55**: 5577; YEH T W, LI H N. Phys. Rev. D, 1997, **56**: 1615
14 LI H N. Prog.Part.& Nucl.Phys., 2003, **51**: 85
15 Lepage G P, Brodsky S J. Phys. Rev. D, 1980, **22**: 2157
16 LI H N. Phys. Rev. D, 2002, **66**: 094010
17 Buchalla G, Buras A J, Lautenbacher M E. Rev. Mod. Phys., 1996, **68**: 1125
18 LÜ C D, Ukai K, YANG M Z. Phys. Rev. D, 2001, **63**: 074009
19 LIU X, WANG H S, XIAO Z J et al. Phys. Rev. D, 2006, **73**: 074002
20 GUO D Q, CHEN X F, XIAO Z J. Phys. Rev. D, 2007, **75**: 054033
21 Feldmann T. Int. J. Mod. Phys. A, 2000, **15**: 159
22 CHARNG Y Y, Kurimoto T, LI H N. Phys. Rev. D, 2006, **74**: 074024; Phys. Rev. D, 2008, **78**: 059901(E)
23 XIAO Z J, ZHANG Z Q, LIU X, GUO L B. Phys. Rev. D, 2008, **78**: 114001
24 Ali A, Kramer G, LÜ C D. Phys. Rev. D, 1998, **58**: 094009
25 LI R H, LÜ C D, WANG W, WANG X X. Phys. Rev. D, 2009, **79**: 014013
26 SHEN Y L. private communication.
27 Heavy Flavor Averaging Group, Barberio E et al. hep-ex/0808.1297 v1; and online update at http://www.slac.stanford.edu/xorg/hfag.
28 Particle Data Group. Phys. Lett. B, 2008, **667**: 1